Hindawi
Journal of Nanomaterials
Volume 2018, Article ID 2603712, 6 pages
https://doi.org/10.1155/2018/2603712

Research Article

Doxorubicin-Loaded Melanin Particles for Enhanced Chemotherapy in Drug-Resistant Anaplastic Thyroid Cancer Cells

Kun Wang[1], **Shouju Wang**[2], **Kun Chen**[1], **Yijing Zhao**[1], **Xingqun Ma**[3] and **Lin Wang**[3]

[1]*Department of Endocrinology, The Affiliated Jiangning Hospital of Nanjing Medical University, Nanjing 211100, China*
[2]*Department of Medical Imaging, Jinling Hospital, School of Medicine, Nanjing University, Nanjing 210000, China*
[3]*Department of Oncology, The Affiliated Bayi Hospital of Nanjing University of Chinese Medicine, Nanjing 210002, China*

Correspondence should be addressed to Kun Wang; doc_kunwang@163.com

Received 19 October 2017; Revised 10 January 2018; Accepted 17 January 2018; Published 11 February 2018

Academic Editor: Ester Vazquez

Anaplastic thyroid cancer (ATC) is highly aggressive and tends to develop drug resistance to standard chemotherapies. To overcome the drug resistance of ATC, we synthesized dopamine-melanin nanoparticles (MNPs) loaded with doxorubicin (Dox) molecules. The Dox-loaded MNPs (Dox-MNPs) developed exhibited increased cellular uptake and enhanced therapeutic efficacy in drug-resistant ATC cell line HTh74R, compared with free Dox. The native MNPs were found to have excellent biocompatibility, which suggests that Dox-MNPs may have potential in the treatment of ATC.

1. Introduction

Anaplastic thyroid cancer (ATC) is a form of thyroid cancer that has one of the highest mortality rates of any cancer [1]. The overall 5-year survival rate of patients with ATC is as low as 7% [2]. The standard treatment for this highly aggressive cancer is a combination of doxorubicin (Dox) chemotherapy and radiation therapy [3]. However, malignant ATC cells often develop resistance to Dox, resulting in failure of the treatment [4, 5]. Overcoming the drug resistance of cells is therefore essential for improving the prognosis of ATC.

A key mechanism in the drug resistance of ATC is related to the expression of multidrug-resistant 1 (MDR1) transporters [6]. MDR1 transporters pump Dox molecules out of cells, reducing the intracellular concentration of the drug and inhibiting the chemotherapeutic efficacy [4, 7]. Recently, significant effort has been directed towards overcoming the drug resistance of cancer cells using nanoparticles as drug carriers [8, 9]. Nanoparticles can deliver drugs with high efficacy and boost intracellular drug concentration by increasing cellular uptake or by inhibiting drug efflux. Several reports have recently demonstrated the feasibility of using nanocarriers, such as liposomes [10] and nanosponges [11], to deliver drugs to enhance their therapeutic efficacy towards ATC. However, to the best of our knowledge, there are no reports demonstrating the potential of using nanoparticles to overcome drug resistance in ATC.

In this work, we synthesized dopamine-melanin nanoparticles (MNPs) for Dox loading. Melanin is a pigment present in a number of human tissues, such as skin, hair, and eyes and has excellent biocompatibility [12–15]. Dox molecules can be adsorbed onto the surface of MNPs by electrostatic interaction and/or π-π stacking [16]. The cellular uptake and therapeutic efficacy of the obtained Dox-loaded MNPs (Dox-MNPs) were investigated in two ATC cells lines: drug-sensitive HTh74 and drug-resistant HTh74R cells.

2. Materials and Methods

2.1. Materials. Dopamine hydrochloride, ethanol, and 2,5-diphenyltetrazolium bromide (MTT) were purchased from Sigma-Aldrich. Doxorubicin, aqueous ammonia (28%–30%), and dimethyl sulfoxide (DMSO) were purchased from

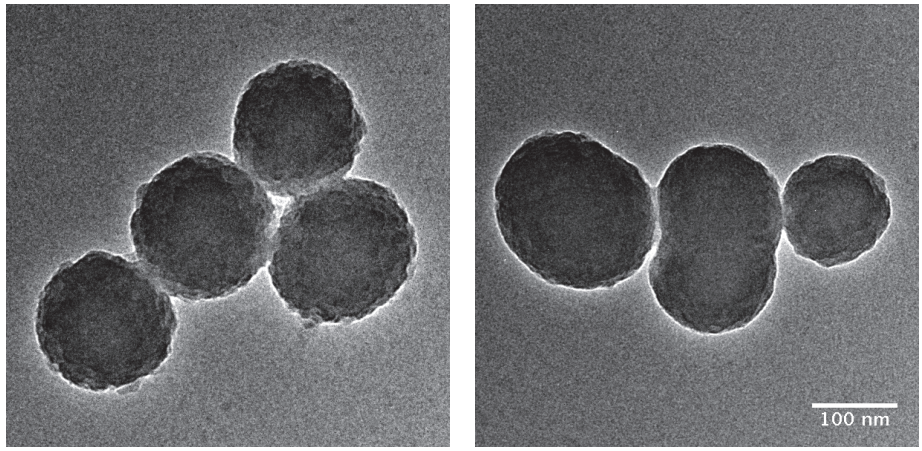

(a) (b)

Figure 1: TEM image of (a) MNPs and (b) Dox-MNPs.

Aladdin Reagent. UltraCruz mounting medium with 4′,6-diamidino-2-phenylindole (DAPI) was purchased from Santa Cruz. Cells were cultured in F-12 medium with 1% 100x minimum essential medium (MEM), 1% amphotericin, 1% 500x penicillin and streptomycin, and 10% fetal calf serum. Phosphate buffered saline (PBS) was purchased from Keygentec.

2.2. Synthesis of MNPs. The MNPs were synthesized as previously reported. Briefly, 8 mL of ethanol and 0.6 mL of aqueous ammonia were mixed with 18 mL of ultrapure water and stirred in a water bath at 30°C for at least 30 min. 2 mL of 50 mg/mL dopamine hydrochloride was then added to the mixture and stirring was continued for 24 h. The solution was subsequently centrifuged three times (15 min, 10000 rpm). The supernatant was carefully discarded after each cycle of centrifugation and the sedimented particles were collected and redispersed in ultrapure water at a concentration of 1 mg/mL for further use.

2.3. Loading Dox onto MNPs. To load Dox onto the surface of the obtained MNPs, a solution of Dox (0.5 mg/mL) was mixed with the MNP suspension detailed in Section 2.2, at various mass ratios from 0.167 : 1 to 2 : 1 (Dox to MNPs). The mixtures were stirred vigorously for 24 h at room temperature, followed by two centrifugation and resuspension steps (15 min, 13000 rpm). The amount of free Dox in the supernatant was determined by UV-Vis spectroscopy to establish the loading efficiency and capacity of MNPs at different mass ratios of Dox to MNPs. Dox-MNPs were redispersed in ultrapure water for further use.

2.4. Characterization of Nanoparticles. Transmission electron microscopy (TEM) images of the MNPs were acquired using a JEOL JEM-2100 microscope. UV-Vis spectra of the MNPs were measured using a PerkinElmer Lambda 35 UV-Vis spectrophotometer. The size and zeta potential of the nanoparticles were measured using a Brookhaven Zeta PALS analyzer.

2.5. MTT Assays. HTh74 and HTh74R cells were cultured in 96-well plates at 37°C in 5% CO_2 for 24 h. The cells were subsequently incubated with various concentrations of free Dox, MNPs, and Dox-MNPs for a further 24 h. Following incubation cells were washed three times with cold PBS, cultured with 0.5 mg/mL MTT for 4 h, and suspended in DMSO. The cell viability was determined by the absorbance of dissolved formazan at 570 nm.

2.6. Flow Cytometry Studies. HTh74, HTh74R, and HEK 293 cells were cultured in 12-well plates at 37°C in 5% CO_2 for 24 h and subsequently incubated with free Dox (40 μg/mL) or Dox-MNPs with the equivalent effective Dox concentration, for 6 h. The cells were then washed three times with cold PBS and collected and redispersed in PBS. The Dox fluorescence signal was recorded using a Cytoflow cytometer.

2.7. Statistical Analysis. Data were analyzed using GraphPad Prism 7.0. The difference in viability between two groups of cells was compared using Student's t-test. A p value of 0.05 was considered the significant threshold.

3. Results and Discussion

The MNPs were successfully synthesized according to method described in Section 2.2. The TEM images show that the obtained MNPs were quasispherical nanoparticles with a diameter of 148.9 ± 13.3 nm (Figure 1(a)). The size and morphology of the obtained MNPs were similar to those of melanin particles produced in the human body. The hydrodynamic diameter was found to be 215.7 ± 5.8 nm, which is slightly larger than the size measured from the TEM images. Dynamic light scattering (DLS) measurement showed that the MNPs had a negative zeta potential of −25.3 ± 3.2 mV, which is suitable for loading of the positively charged Dox molecules.

It has been reported that Dox molecules can adhere to the surface of MNPs through strong π-π stacking and

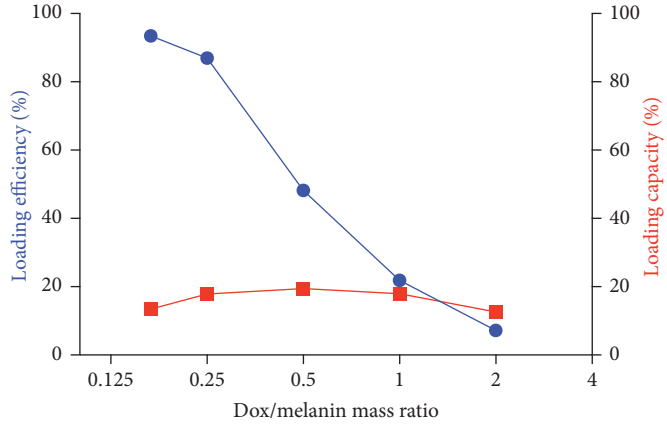

Figure 2: Loading efficiency and loading capacity of Dox-MNPs at different mass ratios of Dox to MNPs.

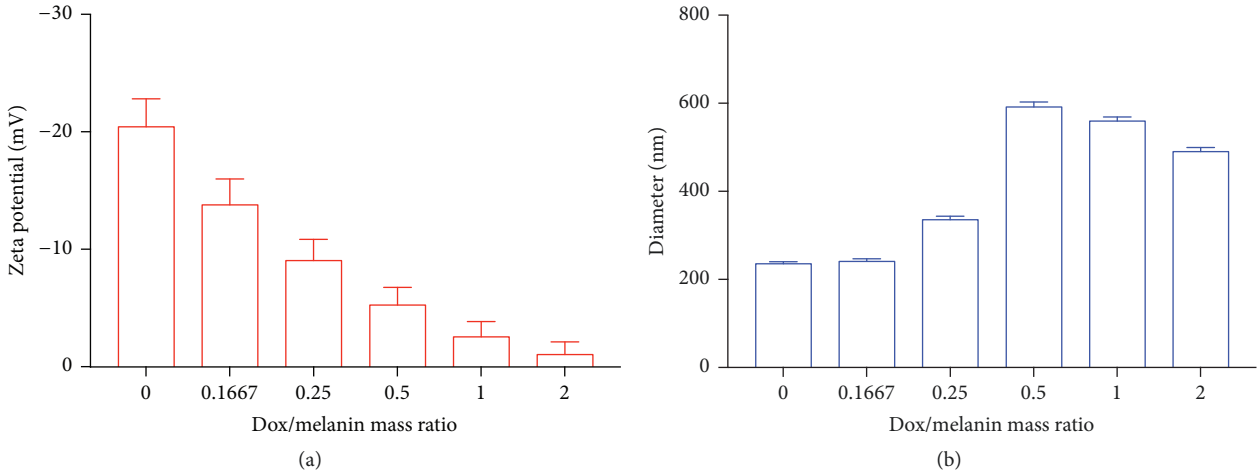

Figure 3: Zeta potential and hydrodynamic diameter of Dox-MNPs at different mass ratios of Dox to MNPs.

hydrogen bonding interactions. To determine their drug loading capability, the MNPs were mixed with Dox at various mass ratios. As shown in Figure 2, the loading efficiency of Dox-MNPs decreased with the increasing mass ratio of Dox to MNPs. The loading efficacy peaked at 93.45% when the mass ratio was 0.167 : 1. However, the loading capacity of Dox-MNPs stabilized between 12.64 and 19.43% regardless of the change in mass ratios.

One challenge of successful drug loading is to identify the appropriate mass ratio of drug to carrier, such that the nanoparticles can retain colloidal stability after drug loading, with minimal interparticle bridging [17]. To optimize the mass ratio for drug loading, the hydrodynamic diameter and zeta potential of Dox-MNPs obtained at different mass ratios were measured. As shown in Figure 3(a), the zeta potential of Dox-MNPs decreased with the increasing mass ratio of Dox to MNPs. At mass ratios greater than 0.25 : 1, the zeta potential of the obtained Dox-MNPs tended from negative to neutral. In parallel with the change in zeta potential, the hydrodynamic diameters of Dox-MNPs increased with the rising mass ratio of Dox to MNPs (Figure 3(b)). Taken together, these results indicate that the Dox-MNPs showed aggregation at the higher mass ratios of Dox to MNPs because the repulsive force between the negatively charged nanoparticles weakened when positively charged Dox molecules were loaded. Since colloidal stability is crucial for the biomedical application of nanoparticles, the mass ratio of Dox to MNPs was optimized at 0.167 : 1 for the subsequent experiments. TEM images showed that, at this mass ratio, the obtained Dox-MNPs had similar morphology to MNPs (Figure 1(b)). DLS measurement revealed the zeta potential and size distribution of Dox-MNPs were −13.79 mV and 241.1 ± 4.8 nm, respectively, at this optimized mass ratio.

Since melanin is the pigment that colors human skin, hair, and eyes, the MNPs were expected to have good biocompatibility. To estimate MNP biocompatibility, HTh74 and HTh74R cells were incubated with various concentrations of MNPs for 24 h. The MTT assays demonstrated that MNPs did not cause significant cytotoxicity at concentrations lower than 450 mg/L (Figure 4).

After establishing the biocompatibility of MNPs, the therapeutic efficacy of free Dox was compared with that of Dox-MNPs in HTh74 and HTh74R cells, based on a constant Dox concentration. As shown in Figure 5, the viability of HTh74

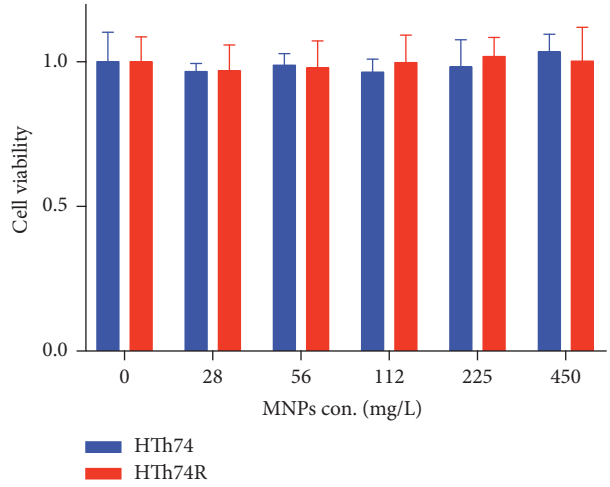

Figure 4: Cell viability of HTh74 and HTh74R after incubation with various concentrations of MNPs for 24 h.

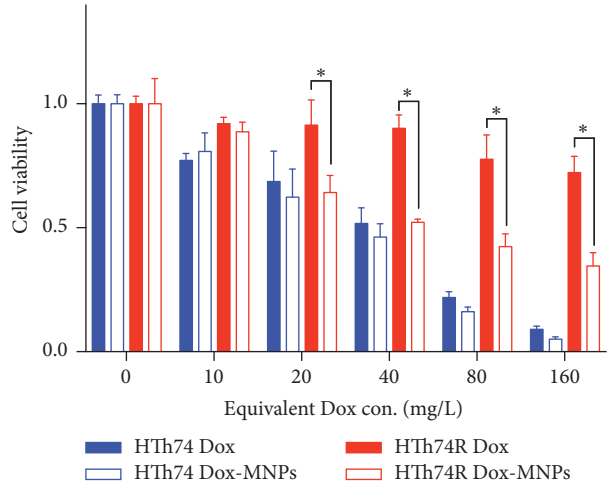

Figure 5: Cell viability of HTh74 and HTh74R after incubation with various concentrations of Dox-MNPs for 24 h.

cells was similar after incubation with free Dox and Dox-MNPs at the equivalent Dox concentration. This indicates that the Dox-MNPs did not enhance the therapeutic efficacy of Dox for drug-sensitive ATC cells. In contrast, for HTh74R cells, Dox-MNPs induced significantly higher therapeutic efficacy than the same amount of free Dox, at concentrations higher than 20 mg/L. At the highest tested concentration (160 mg/L), the viability of HTh74R cells incubated with free Dox was 72.3 ± 6.5%, whereas the viability of HTh74R cells incubated with Dox-MNPs decreased to 34.6 ± 5.4%, suggesting that Dox-MNPs could significantly inhibit the drug resistance of HTh74R cells.

To understand the mechanisms of the enhanced therapeutic efficacy of Dox-MNPs, the cellular uptake of free Dox and Dox-MNPs was compared between HTh74 and HTh74R cells. The fluorescence-activated cell sorting (FACS) results showed that the degree of uptake of free Dox and Dox-MNPs was similar in HTh74 cells (Figure 6(a)). When incubated with HTh74R cells, the uptake of free Dox was lower than when incubated with HTh74 cells, indicating that the drug resistance of HTh74R cells was related to poor Dox internalization. It is noted that the degree of uptake of Dox-MNPs in HTh74R cells was similar to that in HTh74 cells (Figure 6(b)), suggesting that Dox-MNPs could be internalized by HTh74R cells more efficiently than free Dox, resulting in enhanced chemotherapeutic efficacy. To further exclude the possibility that Dox-MNPs would enhance the cell uptake of Dox in normal cells, the cellular uptake of free Dox and Dox-MNPs in HEK 293 cells was also determined. The FACS data show that the degree of uptake of free Dox and Dox-MNPs was similar in HEK 293 cells (Figure 7), indicating that the drug-induced toxicity for normal cells would not be enhanced by the MNP drug delivery system.

4. Conclusions

In summary, we constructed dopamine-melanin nanoparticles for high efficiency loading of Dox (93.45%). The cellular uptake and therapeutic efficacy of the Dox-loaded dopamine-melanin nanoparticles were significantly higher than those of

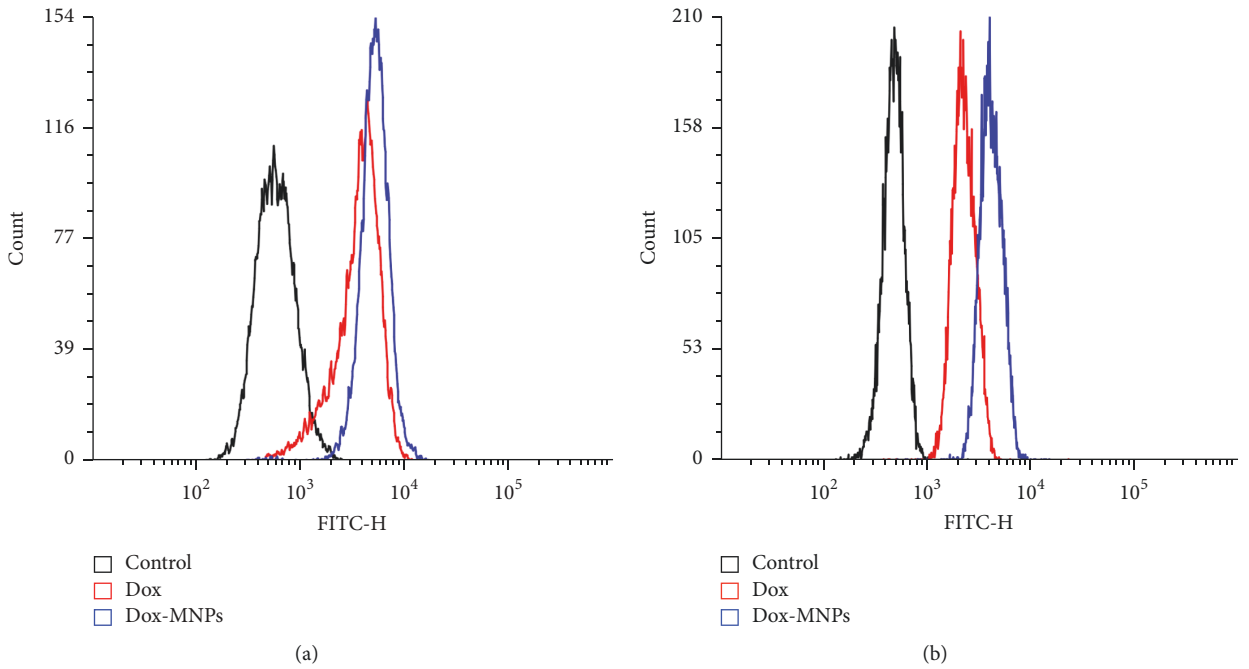

Figure 6: Intracellular Dox fluorescent signal of control cells and cells incubated with free Dox or Dox-MNPs for 6 h in (a) HTh74 and (b) HTh74R cells.

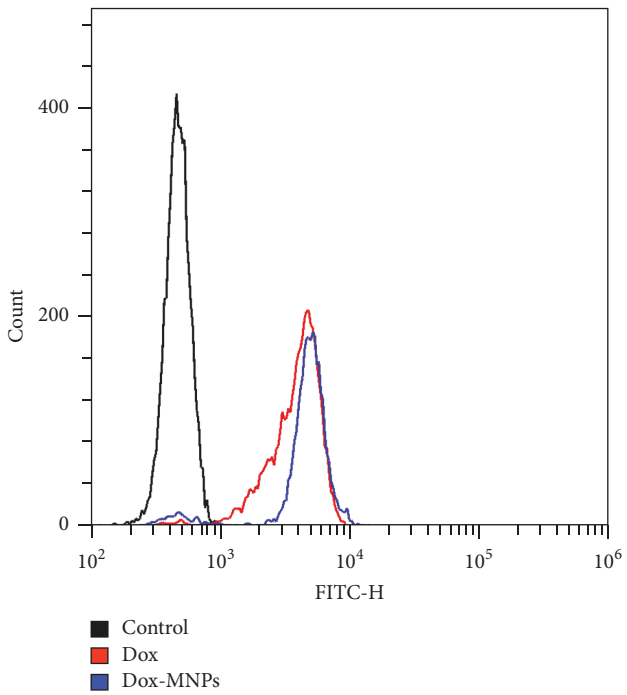

Figure 7: Intracellular Dox fluorescent signal of control cells and cells incubated with free Dox or Dox-MNPs for 6 h in HEK 293 cells.

free Dox at the same drug concentration, in drug-resistant HTh74R cells. To the best of our knowledge, this is the first report demonstrating that dopamine-melanin nanoparticles could be used to overcome the drug resistance of anaplastic thyroid cancer cells.

Conflicts of Interest

The authors declare that there are no conflicts of interest regarding the publication of this paper.

Authors' Contributions

Kun Wang and Shouju Wang contributed equally to this paper.

Acknowledgments

This project is financially supported by the Natural Science Foundation of China (Program no. 81501588), the Natural Science Foundation of Jiangsu Province (Program no. BK20140734), and the Doctoral Graduate Innovation Fund in Affiliated Nanjing Jiangning Hospital of Nanjing Medical University. The authors thank Sarah Dodds, Ph.D., from Liwen Bianji, Edanz Editing, China (https://www.liwenbianji.cn/ac), for editing the English text of a draft of this manuscript.

References

[1] L. Davies and H. G. Welch, "Increasing incidence of thyroid cancer in the United States, 1973–2002," *Journal of the American Medical Association*, vol. 295, no. 18, pp. 2164–2167, 2006.

[2] R.-Y. Lin, "Thyroid cancer stem cells," *Nature Reviews Endocrinology*, vol. 7, no. 10, pp. 609–616, 2011.

[3] E. Molinaro, C. Romei, A. Biagini et al., "Anaplastic thyroid carcinoma: From clinicopathology to genetics and advanced

therapies," *Nature Reviews Endocrinology*, vol. 13, no. 11, pp. 644–660, 2017.

[4] P. J. Davis, S. Incerpi, H.-Y. Lin, H.-Y. Tang, T. Sudha, and S. A. Mousa, "Thyroid hormone and P-glycoprotein in tumor cells," *BioMed Research International*, vol. 2015, Article ID 168427, 2015.

[5] X. Zheng, D. Cui, S. Xu, G. Brabant, and M. Derwahl, "Doxorubicin fails to eradicate cancer stem cells derived from anaplastic thyroid carcinoma cells: Characterization of resistant cells," *International Journal of Oncology*, vol. 37, no. 2, pp. 307–315, 2010.

[6] C. Massart, C. Poirier, P. Fergelot, O. Fardel, and J. Gibassier, "Effect of sodium butyrate on doxorubicin resistance and expression of multidrug resistance genes in thyroid carcinoma cells," *Anti-Cancer Drugs*, vol. 16, no. 3, pp. 255–261, 2005.

[7] G. Chen, S. Xu, K. Renko, and M. Derwahl, "Metformin inhibits growth of thyroid carcinoma cells, suppresses self-renewal of derived cancer stem cells, and potentiates the effect of chemotherapeutic agents," *The Journal of Clinical Endocrinology & Metabolism*, vol. 97, no. 4, pp. E510–E520, 2012.

[8] L. Zeng, Y. Pan, Y. Tian et al., "Doxorubicin-Loaded $NaYF_4$:Yb/Tm–TiO_2 Inorganic Photosensitizers for NIR-Triggered Photodynamic Therapy and Enhanced Chemotherapy in Drug-Resistant Breast Cancerscancers," *Biomaterials*, vol. 57, pp. 93–106, 2015.

[9] X. Wang, Y. Liu, S. Wang et al., "CD44-engineered mesoporous silica nanoparticles for overcoming multidrug resistance in breast cancer," *Applied Surface Science*, vol. 332, pp. 308–317, 2015.

[10] M. C. Cristiano, D. Cosco, C. Celia et al., "Anticancer activity of all-trans retinoic acid-loaded liposomes on human thyroid carcinoma cells," *Colloids and Surfaces B: Biointerfaces*, vol. 150, pp. 408–416, 2017.

[11] C. L. Gigliotti, B. Ferrara, S. Occhipinti et al., "Enhanced cytotoxic effect of camptothecin nanosponges in anaplastic thyroid cancer cells in vitro and in vivo on orthotopic xenograft tumors," *Drug Delivery*, vol. 24, no. 1, pp. 670–680, 2017.

[12] Y. Liu, K. Ai, J. Liu, M. Deng, Y. He, and L. Lu, "Dopamine-melanin colloidal nanospheres: An efficient near-infrared photothermal therapeutic agent for in vivo cancer therapy," *Advanced Materials*, vol. 25, no. 9, pp. 1353–1359, 2013.

[13] X. Wang, J. Zhang, Y. Wang et al., "Multi-responsive photothermal-chemotherapy with drug-loaded melanin-like nanoparticles for synergetic tumor ablation," *Biomaterials*, vol. 81, pp. 114–124, 2016.

[14] Q. Fan, K. Cheng, X. Hu et al., "Transferring biomarker into molecular probe: Melanin nanoparticle as a naturally active platform for multimodality imaging," *Journal of the American Chemical Society*, vol. 136, no. 43, pp. 15185–15194, 2014.

[15] A. Liopo, R. Su, and A. A. Oraevsky, "Melanin nanoparticles as a novel contrast agent for optoacoustic tomography," *Photoacoustics*, vol. 3, no. 1, pp. 35–43, 2015.

[16] W.-Q. Li, Z. Wang, S. Hao et al., "Mitochondria-Targeting Polydopamine Nanoparticles to Deliver Doxorubicin for Overcoming Drug Resistance," *ACS Applied Materials & Interfaces*, vol. 9, no. 20, pp. 16793–16802, 2017.

[17] S. Wang, Y. Tian, W. Tian et al., "Selectively Sensitizing Malignant Cells to Photothermal Therapy Using a CD44-Targeting Heat Shock Protein 72 Depletion Nanosystem," *ACS Nano*, vol. 10, no. 9, pp. 8578–8590, 2016.